Coupled stress and energy criterion for multiple matrix cracking in cross-ply composite laminates

M. Kashtalyan*[1], I.G. García[2] and V. Mantič[2]

[1]School of Engineering, University of Aberdeen, Scotland UK, m.kashtalyan@abdn.ac.uk,

[2]School of Engineering, University of Seville, Spain, israelgarcia@us.es, mantic@us.es

* Corresponding author

Abstract.

Transverse cracking, i.e. matrix cracking in the off-axis plies of the laminate, is widely recognized as the first damage mode to appear in continuous fibre-reinforced composite laminates subjected to in-plane loading. Since transverse cracking has a great influence on the subsequent damage steps such as delaminations or oblique cracks, it is important to be able to predict its onset and growth accurately. In this paper, it is proposed to use a combination of the Coupled Criterion of Finite Fracture Mechanics (FFM) and the Equivalent Constraint Model (ECM) to predict the evolution of crack density with increasing applied load. Two formulations – a discrete formulation and a continuous formulation – are developed for the energy criterion within the Coupled Criterion. Some dependences between the two formulations are proved, which justifies the good agreement found by the models based on continuous formulations presented by other authors despite the inherent discrete nature of the phenomenon. Dependence of the failure load predicted by the Coupled Criterion on the layer thickness ratio and brittleness number (a structural parameter that characterizes a combination of stiffness, strength, fracture toughness and the thickness of the cracked ply of the laminate) is examined and discussed for carbon/epoxy and glass/epoxy laminates. Finally, comparison against experimental results shows a good agreement.

Keywords: transverse cracking, composite laminate, failure criterion, finite fracture mechanics

1. Introduction

Failure of continuous fibre-reinforced composite laminates subjected to in-plane loading involves sequential accumulation of various type of damage. The first damage mode to appear is usually transverse cracking, i.e. matrix cracking in the off-axis plies of the laminate. Transverse cracking

reduces the laminate stiffness and triggers development of other damage modes such as delaminations. It is therefore important to be able to predict accurately the onset and evolution of transverse cracking.

Transverse cracking in composite laminates has been the subject of extensive research, see reviews by Nairn (2000), Berthelot (2003), Kashtalyan and Soutis (2005).

Garrett and Bailey (1977) were arguably the first to propose to use maximum stress criterion for predicting the initiation of matrix cracking in cross-ply laminates. However, stress-based approaches do not agree well with experimental data which show that onset of matrix cracking strongly depends on the laminate structure. Subsequent developments in this direction involved using more sophisticated failure criteria, as well as taking into account the probabilistic and statistical nature of strength, see reviews by Silberschmidt (2005) and Singh (2016).

Recognizing limitations of strength-based models, Parvizi et al (1978) proposed to use an energy criterion to predict the initiation of transverse cracking. According to this criterion, the first crack forms when the energy release rate associated with its formation exceeds some critical value. This critical value may be taken as G_{Ic}, the Mode I transverse fracture toughness (Cepero et al, 2014), or G_{mc}, the microcracking fracture toughness (Nairn, 2000). However, more research is required to confirm that G_{mc} is a material property, independent of the laminate stacking sequence. Caslini et al (1987) suggested to use the energy release rate for predicting the development of transverse cracking. They predicted transverse crack density as a function of applied load, treating the total area of transverse cracks as continuous variable and deriving analytical expressions for the strain energy release rate and its derivative. Laws and Dvorak (1988) and Nairn (1989) recognized the discrete nature of transverse crack formation and estimated the energy released during the formation of a new transverse cracks between two existing transverse cracks, using a one-dimensional shear-lag and a variational approach, respectively. Zhang, Fan and Soutis (1992b) proposed to use the resistance curve concept with the energy criterion in order to capture the experimental observation that it becomes more difficult for new transverse cracks to form as the transverse crack density increases.

In the last decades, Finite Fracture Mechanics (FFM) (Hashin, 1996) has emerged as a novel approach that aims to address the limitations of Classical Linear Fracture Mechanics which can only deal with the growth of pre-existing cracks (see review by Weiβgraeber et al. 2016). The FFM concept assumes the instantaneous formation of cracks of finite size at initiation. Within the framework of FFM, Leguillon (2002) proposed a coupled stress and energy criterion to identify the critical loading and the corresponding crack size. As an application of this Coupled Criterion, first, initiation of transverse cracking in fibre-reinforced composites was investigated by Mantič (2009) and Mantič and García (2012), who examined crack onset and growth at fibre/matrix interface under transverse tension and biaxial load, respectively, assuming dilute fibre packing so that the influence of neighbouring fibres can be neglected. Second, García et al. (2014) investigated transverse cracking onset and growth in cross-ply laminates under tension, focusing on formation of the very first crack within the 90^o ply and studying its growth within that ply. More recently, multiple cracking in cross-ply laminate using FFM and numerical modelling has been examined by Leguillon et al. (2017) and Li and Leguillon (2017).

In this work, we extend Leguillon's Coupled Criterion of FFM (Leguillon, 2002) to multiple transverse cracking in composite laminates. The plies are assumed to be homogeneous, therefore the processes inherent to the heterogeneities at the micro scale (e.g. in Aerteiro et al. (2014), Herráez et al. (2015), Saito et al. (2014), Távara et al (2017)) are not introduced explicitly in this analysis. The objective of this work is the prediction of the evolution of crack density with the increasing external load. The relationship between the evolution of crack density and the external load is predicted by the combination of the Coupled Criterion and the Equivalent Constraint Model (ECM) (Kashtalyan and Soutis, 2000; 2006). Thanks to the ECM, which provides analytical expressions for the energy released by the onset of a transverse crack in a damaged laminate and the stresses inside it, the applications of the Coupled Criterion can provide a semi-analytical expression relating the evolution of crack density and the external load.

This paper describes in Sections 2 and 3 how the ECM is used to obtain closed-form expression for the stresses in the cracked laminate and its effective stiffness as a function of the crack density. Based on this expressions, in Section 4 the conditions given by the stress and energy criteria for the crack density progression are presented. The main results are discussed in Section 5. Finally, a comparison with experiments is presented in Section 6.

2. Stress analysis

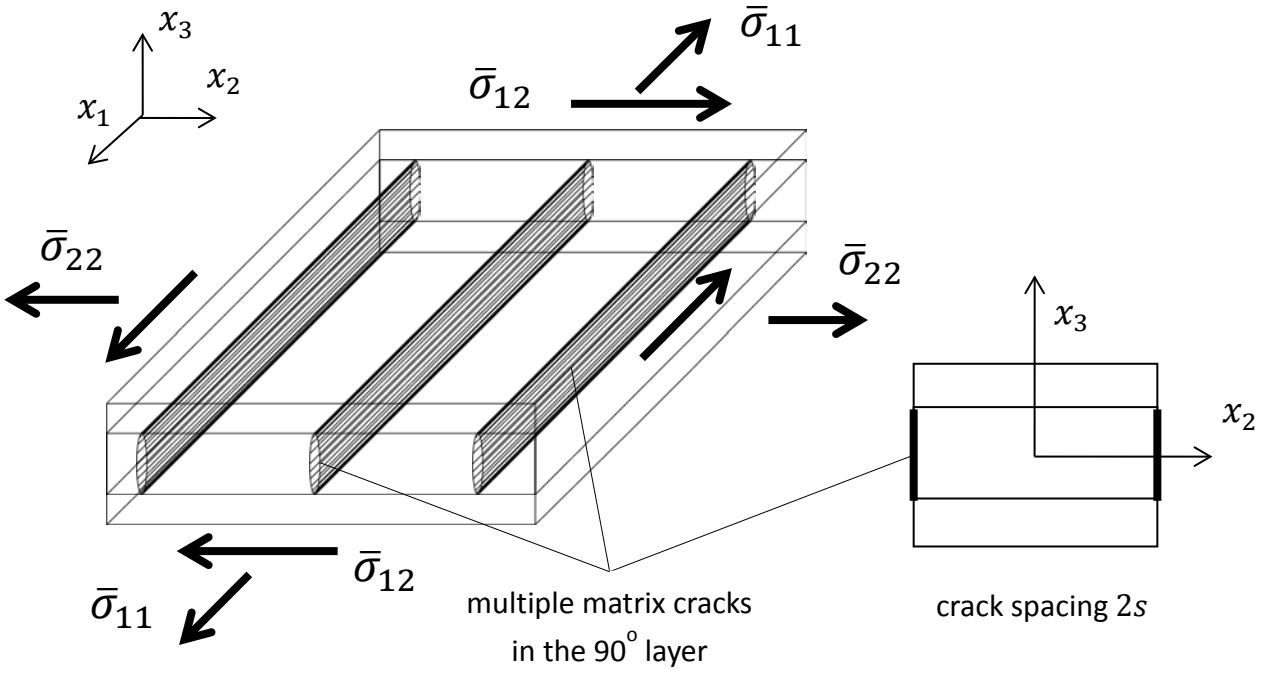

Figure 1. Schematic representation of a cross-ply laminate with multiple matrix cracks in the 90° layer.

Consider a symmetric cross-ply $[0°/90°]_s$ composite laminate that consists of a 90° layer of thickness $2t_{90}$ fully bonded between two 0° layers of thickness t_0. The inner 90° layer contains multiple transverse cracks spanning the full thickness of the inner layer and width $2w$ of the laminate. The cracks are assumed to be spaced uniformly with crack spacing $2s$. The laminate is referred to the co-ordinate system $x_1x_2x_3$, with x_1 axis parallel to the cracks (Fig. 1) and subjected to biaxial tension $\bar{\sigma}_{11}, \bar{\sigma}_{22}$ and in-plane shear loading $\bar{\sigma}_{12}$. Due to periodicity of damage and symmetry of the sample, only a quarter of the representative segment bounded by two cracks (Fig. 1) needs to be considered in the analysis.

The equilibrium equations in terms of ply stresses, averaged across the thickness of the layer and the depth of the laminate, have the form

$$\chi\tilde{\sigma}_{ij}^{(0)} + \tilde{\sigma}_{ij}^{(90)} = (1+\chi)\sigma_{ij}, \quad i,j = 1,2, \quad \chi = t_0/t_{90}, \tag{1a}$$

$$\frac{d\tilde{\sigma}_{22}^{(90)}}{dx_2}+\frac{\tau_2}{t_{90}}=0, \qquad \frac{d\tilde{\sigma}_{12}^{(90)}}{dx_2}+\frac{\tau_1}{t_{90}}=0, \tag{1b}$$

$$\tilde{\sigma}_{ij}^{(90)}=\frac{1}{4wt_{90}}\int_{-w}^{w}\int_{-t_{90}}^{t_{90}}\sigma_{ij}^{(90)}(x_1,x_2,x_3)dx_1dx_3, \tag{1c}$$

where τ_1,τ_2 are the interface shear stresses at the 0°/90° interface.

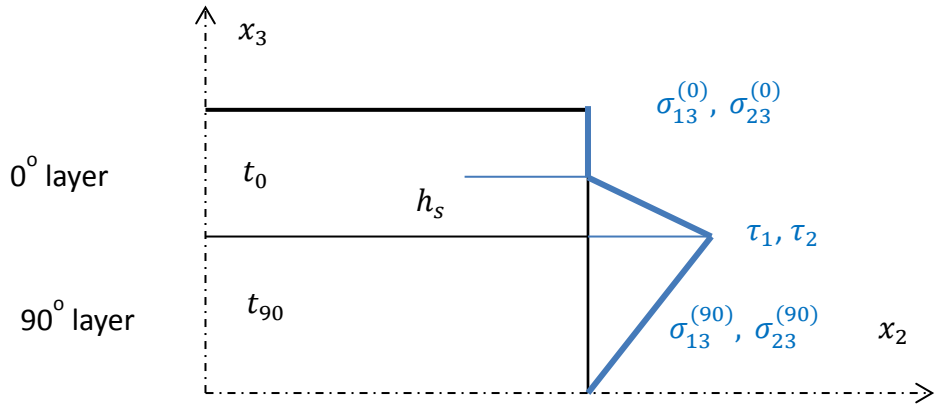

Figure 2. Schematic of the assumptions made for the stress distribution along the laminate thickness.

It is assumed that out-of-plane shear stresses vary linearly with x_3 in each ply but in the outer 0° layer this variation is restricted to the shear layer of thickness h_s (Fig. 2), so that

$$\begin{aligned}&\sigma_{j3}^{(90)}=\frac{\tau_j}{t_{90}}x_3, \quad |x_3|<t_{90};\\ &\sigma_{j3}^{(0)}=\frac{\tau_j}{h_s}(t_{90}+h_s-x_3), \quad t_{90}<|x_3|<t_{90}+h_s, \quad j=1,2.\end{aligned} \tag{2}$$

The interface shear stresses τ_1,τ_2 can be expressed in terms of the in-plane displacements $\tilde{u}_j^{(90)},\tilde{u}_j^{(0)}$, $j=1,2$, and shear moduli $G_{j3}^{(0)},G_{j3}^{(90)}$ of the unidirectional material as

$$\begin{aligned}&\tau_j=K_j(\tilde{u}_j^{(0)}-\tilde{u}_j^{(90)}), \quad K_j=\frac{3G_{j3}^{(0)}G_{j3}^{(90)}}{t_{90}G_{j3}^{(0)}+(1+(1-\eta)/2)\eta t_0G_{j3}^{(90)}}, \quad \eta=h_s/t_0,\\ &\tilde{u}_j^{(0)}=\frac{1}{2wt_0}\int_{-w}^{w}\int_{t_{90}}^{t_{90}+t_0}u_j^{(0)}(x_1,x_2,x_3)dx_1dx_3, \quad \tilde{u}_j^{(90)}=\frac{1}{4wt_{90}}\int_{-w}^{w}\int_{-t_{90}}^{t_{90}}u_j^{(90)}(x_1,x_2,x_3)dx_1dx_3.\end{aligned} \tag{3}$$

The constitutive equations in terms of ply strains and ply stresses are

$$\begin{bmatrix}\widetilde{\varepsilon}_{11}^{(90)}\\ \widetilde{\varepsilon}_{22}^{(90)}\\ \widetilde{\gamma}_{12}^{(90)}\end{bmatrix}=\begin{bmatrix}S_{11}^{(90)} & S_{12}^{(90)} & 0\\ S_{12}^{(90)} & S_{22}^{(90)} & 0\\ 0 & 0 & S_{66}^{(90)}\end{bmatrix}\begin{bmatrix}\widetilde{\sigma}_{11}^{(90)}\\ \widetilde{\sigma}_{22}^{(90)}\\ \widetilde{\sigma}_{12}^{(90)}\end{bmatrix},\qquad \begin{bmatrix}\widetilde{\varepsilon}_{11}^{(0)}\\ \widetilde{\varepsilon}_{22}^{(0)}\\ \widetilde{\gamma}_{12}^{(0)}\end{bmatrix}=\begin{bmatrix}S_{11}^{(0)} & S_{12}^{(0)} & 0\\ S_{12}^{(0)} & S_{22}^{(0)} & 0\\ 0 & 0 & S_{66}^{(0)}\end{bmatrix}\begin{bmatrix}\widetilde{\sigma}_{11}^{(0)}\\ \widetilde{\sigma}_{22}^{(0)}\\ \widetilde{\sigma}_{12}^{(0)}\end{bmatrix} \tag{4a}$$

$$\widetilde{\varepsilon}_{ij}^{(90)}=\frac{1}{4wt_{90}}\int_{-w}^{w}\int_{-t_{90}}^{t_{90}}\varepsilon_{ij}^{(90)}(x_1,x_2,x_3)dx_1dx_3,\qquad \widetilde{\varepsilon}_{ij}^{(0)}=\frac{1}{2wt_0}\int_{-w}^{w}\int_{t_{90}}^{t_{90}+t_0}\varepsilon_{ij}^{(0)}(x_1,x_2,x_3)dx_1dx_3. \tag{4b}$$

In addition, it is also assumed that $\widetilde{\varepsilon}_{11}^{(90)}=\widetilde{\varepsilon}_{11}^{(0)}$ associated to the generalized plane strain assumption, and crack surfaces are stress-free, i.e.

$$\widetilde{\sigma}_{22}^{(90)}\Big|_{x_2=\pm s}=0,\quad \widetilde{\sigma}_{12}^{(90)}\Big|_{x_2=\pm s}=0 \tag{5}$$

Equations (1)-(4) can be reduced to two uncoupled second-order ordinary differential equations with respect to in-plane ply stresses in the 90° layer

$$\begin{aligned}&\frac{d^2\widetilde{\sigma}_{22}^{(90)}}{dx_2}-L_1^{(90)}\widetilde{\sigma}_{22}^{(90)}+\Omega_{11}^{(90)}\overline{\sigma}_{11}+\Omega_{22}^{(90)}\overline{\sigma}_{22}=0,\\ &\frac{d^2\widetilde{\sigma}_{12}^{(90)}}{dx_2}-L_2^{(90)}\widetilde{\sigma}_{12}^{(90)}+\Omega_{12}^{(90)}\overline{\sigma}_{12}=0\end{aligned} \tag{6}$$

Solutions of these equations that satisfy boundary conditions, Eqn. (5), can be found as

$$\begin{aligned}&\widetilde{\sigma}_{22}^{(90)}=\frac{1}{L_1^{(90)}}\left(1-\frac{\cosh\sqrt{L_1^{(90)}}x_2}{\cosh\sqrt{L_1^{(90)}}s}\right)(\Omega_{11}^{(90)}\sigma_{11}+\Omega_{22}^{(90)}\sigma_{22}),\\ &\widetilde{\sigma}_{12}^{(90)}=\frac{1}{L_2^{(90)}}\left(1-\frac{\cosh\sqrt{L_2^{(90)}}x_2}{\cosh\sqrt{L_2^{(90)}}s}\right)\Omega_{12}^{(90)}\overline{\sigma}_{12},\end{aligned} \tag{7}$$

where

$$
\begin{aligned}
L_1^{(90)} &= \frac{K_2}{t_0}[S_{22}^{(0)} + \chi S_{22}^{(90)} + a_1(S_{12}^{(0)} + \chi S_{12}^{(90)})],\\
L_2^{(90)} &= \frac{K_1}{t_0}(S_{66}^{(0)} + \chi S_{66}^{(90)}),\\
\Omega_{11}^{(90)} &= \frac{K_2}{t_0}(1+\chi)(S_{12}^{(0)} + a_1 S_{11}^{(0)}),\\
\Omega_{22}^{(90)} &= \frac{K_2}{t_0}(1+\chi)(S_{22}^{(0)} + a_1 S_{12}^{(0)}),\\
\Omega_{12}^{(90)} &= \frac{K_1}{t_0}(1+\chi)S_{66}^{(0)},\\
a_1 &= -\frac{S_{12}^{(0)} + \chi S_{12}^{(90)}}{S_{11}^{(0)} + \chi S_{11}^{(90)}}.
\end{aligned}
\tag{8}
$$

The detailed derivation of the above equations can be found in Kashtalyan and Soutis (2000, 2006, 2013), where a slightly different notation is used.

3. Effective stiffness of the cracked layer

Consider now an equivalent constraint laminate, in which the damaged layer is replaced with an equivalent homogeneous layer with degraded stiffness properties. The constitutive equations of the "equivalent" layer in the co-ordinate system $x_1x_2x_3$ are

$$
\{\bar{\sigma}^{(90)}\} = [\overline{Q}^{(90)}]\{\bar{\varepsilon}^{(90)}\}. \tag{9}
$$

The macrostresses $\{\bar{\sigma}^{(90)}\}$ and macrostrains $\{\bar{\varepsilon}^{(90)}\}$ in the equivalent homogeneous layer can be determined from the in-plane ply stresses $\tilde{\sigma}_{ij}^{(90)}$ and ply strains $\tilde{\varepsilon}_{ij}^{(90)}$ by integrating over the length $2s$ of the representative segment (Fig. 1) as

$$
\bar{\sigma}_{ij}^{(90)} = \frac{1}{2s}\int_{-s}^{s}\tilde{\sigma}_{ij}^{(90)}dx_2, \quad \bar{\varepsilon}_{ij}^{(90)} = \bar{\varepsilon}_{ij}^{(0)} = \bar{\varepsilon}_{ij} = \frac{1}{2s}\int_{-s}^{s}\tilde{\varepsilon}_{ij}^{(90)}dx_2. \tag{10}
$$

where $2s$ is the crack spacing.

The equality between $\bar{\varepsilon}_{ij}^{(90)}$ and $\bar{\varepsilon}_{ij}^{(0)}$ is based on the assumption of generalized plane strain. The reduced in-plane stiffness matrix $[\overline{Q}^{(90)}]$ of the equivalent homogeneous layer is related to the in-

plane stiffness matrix $[\hat{Q}^{(90)}]$ of the undamaged layer via the In-situ Damage Effective Functions (IDEFs) $\Lambda_{22}^{(90)}$, $\Lambda_{66}^{(90)}$ (Zhang, Fan and Soutis, 1992a) as

$$[\overline{Q}^{(90)}]=[\hat{Q}^{(90)}]-[R],\quad [R]\equiv[R(D^{mc})]=\begin{bmatrix} \dfrac{(\hat{Q}_{12}^{(90)})^2}{\hat{Q}_{22}^{(90)}}\Lambda_{22}^{(90)} & \hat{Q}_{12}^{(90)}\Lambda_{22}^{(90)} & 0 \\ \hat{Q}_{12}^{(90)}\Lambda_{22}^{(90)} & \hat{Q}_{22}^{(90)}\Lambda_{22}^{(90)} & 0 \\ 0 & 0 & \hat{Q}_{66}^{(90)}\Lambda_{66}^{(90)} \end{bmatrix} \tag{11}$$

where $D^{mc}=t_{90}/s$ is the relative transverse crack density. The IDEFs $\Lambda_{22}^{(90)}$, $\Lambda_{66}^{(90)}$ can be expressed in terms of macrostresses $\overline{\sigma}_{ij}^{(90)}$ and macrostrains $\overline{\varepsilon}_{ij}^{(90)}$ as

$$\Lambda_{22}^{(90)}=1-\frac{\overline{\sigma}_{22}^{(90)}}{\hat{Q}_{12}^{(90)}\overline{\varepsilon}_{11}^{(90)}+\hat{Q}_{22}^{(90)}\overline{\varepsilon}_{22}^{(90)}},\quad \Lambda_{66}^{(90)}=1-\frac{\overline{\sigma}_{12}^{(90)}}{\hat{Q}_{66}^{(90)}\overline{\varepsilon}_{12}^{(90)}} \tag{12}$$

By substituting Eqn. (7a) into Eqn. (10) and then into Eqn. (12), closed-form expressions for the IDEFs, representing them as explicit functions of the relative transverse crack density $D^{mc}=t_{90}/s$ are obtained

$$\Lambda_{22}^{(90)}=1-\frac{1-\dfrac{D^{mc}}{\lambda_1^{(90)}}\tanh\left[\dfrac{\lambda_1^{(90)}}{D^{mc}}\right]}{1+\alpha_1^{(90)}\dfrac{D^{mc}}{\lambda_1^{(90)}}\tanh\left[\dfrac{\lambda_1^{(90)}}{D^{mc}}\right]}, \tag{13a}$$

$$\Lambda_{66}^{(90)}=1-\frac{1-\dfrac{D^{mc}}{\lambda_2^{(90)}}\tanh\left[\dfrac{\lambda_2^{(90)}}{D^{mc}}\right]}{1+\alpha_2^{(90)}\dfrac{D^{mc}}{\lambda_2^{(90)}}\tanh\left[\dfrac{\lambda_2^{(90)}}{D^{mc}}\right]} \tag{13b}$$

Here the constants $\lambda_i^{(90)}=t_{90}\sqrt{L_i^{(90)}}$ and $\alpha_i^{(90)}$, $i=1,2$, depend solely on the compliances $\hat{S}_{ij}^{(0)}$, $\hat{S}_{ij}^{(90)}$ of the 0° and 90° layers respectively, the shear lag parameters K_j and the layer thickness ratio χ, whereas

$$\alpha_1^{(90)} = \frac{1}{\chi}[\hat{Q}_{22}^{(90)}(\hat{S}_{22}^{(0)} + a_1\hat{S}_{12}^{(0)}) + \hat{Q}_{12}^{(90)}(\hat{S}_{12}^{(0)} + a_1\hat{S}_{11}^{(0)})], \quad \alpha_2^{(90)} = \frac{1}{\chi}\hat{Q}_{66}^{(90)}\hat{S}_{66}^{(0)} \tag{14}$$

The extension stiffness matrix of the equivalent constraint laminate can be calculated as

$$[\overline{A}] = 2[\hat{Q}^{(0)}]t_0 + 2([\hat{Q}^{(90)}] - [R(D^{mc})])t_{90} = [\hat{A}] - 2[R(D^{mc})]t_{90} \tag{15}$$

which relates the laminate macrostresses $\overline{\sigma}_{11}$, $\overline{\sigma}_{22}$ and in-plane shear loading $\overline{\sigma}_{12}$ with the homogenised strains $\overline{\varepsilon}_{11}$, $\overline{\varepsilon}_{22}$ and $\overline{\gamma}_{12}$.

$$\begin{bmatrix} \overline{\sigma}_{11} \\ \overline{\sigma}_{22} \\ \overline{\sigma}_{12} \end{bmatrix} = \frac{1}{2(t_0 + t_{90})} \begin{bmatrix} \overline{A}_{11} & \overline{A}_{12} & 0 \\ \overline{A}_{12} & \overline{A}_{22} & 0 \\ 0 & 0 & \overline{A}_{66} \end{bmatrix} \begin{bmatrix} \overline{\varepsilon}_{11} \\ \overline{\varepsilon}_{22} \\ \overline{\gamma}_{12} \end{bmatrix} \tag{16}$$

4. Coupled criterion for multiple transverse cracking

Formation of more cracks and the corresponding increase in the relative crack density from D_i^{mc} to D_f^{mc} (Fig. 3) may be viewed as a finite fracture event (Hashin, 1996), which, in accordance with the Coupled Criterion (Leguillon, 2002), can occur if both energy criterion and stress criterion are fulfilled.

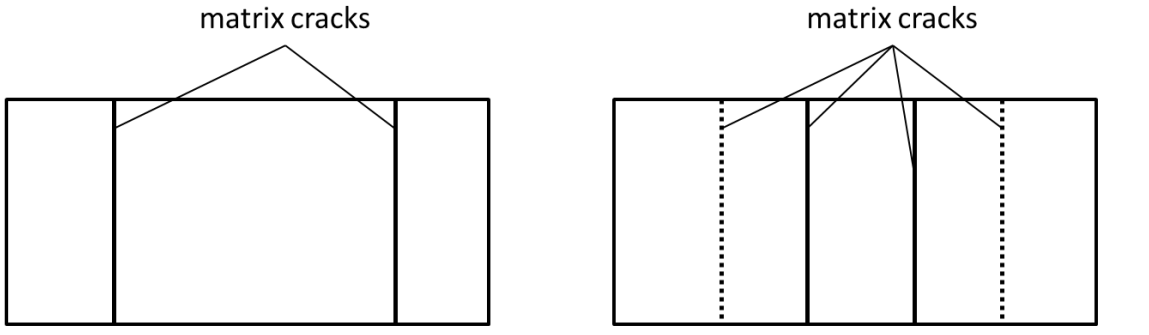

State 1 – laminate with multiple matrix cracks (relative crack density $D_i^{mc} > 0$)

State 2 – laminate with multiple matrix cracks (relative crack density $D_f^{mc} > D_i^{mc}$)

Figure 3. Schematic representation of the laminate with transverse cracks (top view)

According to the maximum stress criterion, new cracks can form between the existing cracks if the following condition for the applied load $\overline{\sigma}_{22}$

$$\tilde{\sigma}_{22}^{(90)} \geq Y_t \quad \Leftrightarrow \quad \frac{1}{L_1^{(90)}}\left(1-\frac{\cosh\sqrt{L_1^{(90)}}x_2}{\cosh\sqrt{L_1^{(90)}}s}\right)\Omega_{22}^{(90)}\overline{\sigma}_{22} \geq Y_t \tag{17}$$

is fulfilled at some position(s) $|x_2|< s$; here Y_t is the transverse tensile strength of the unidirectional lamina, and constants $L_1^{(90)}$ and $\Omega_{22}^{(90)}$ are given by Eq. (8).

The condition expressed in Eq. (17) can be reformulated as a condition for the applied uniaxial strain $\overline{\varepsilon}_{22}$ using Eq. (16) and assuming $\overline{\sigma}_{11}=0$. After some rearrangement, the final expression of the stress criterion is,

$$\frac{\overline{\varepsilon}_{22}}{Y_{\varepsilon t}} \geq \frac{E_{22}L_1^{(90)}}{\Omega_{22}^{(90)}\left(1-\frac{\cosh\sqrt{L_1^{(90)}}x_2}{\cosh\sqrt{L_1^{(90)}}s}\right)}\ \frac{\overline{A}_{11}}{\overline{A}_{11}\overline{A}_{22}-\overline{A}_{12}^2} \tag{18}$$

where $Y_{\varepsilon t}=Y_t/E_{22}$ is the unidirectional critical transverse strain of the lamina and E_{22} is the transverse Young modulus of the lamina.

Assuming that new cracks will appear at the most loaded position, i.e. in the middle between two cracks ($x_2=0$), the previous condition can be specified as

$$\frac{\overline{\varepsilon}_{22}}{Y_{\varepsilon t}} \geq \frac{E_{22}L_1^{(90)}}{\Omega_{22}^{(90)}\left(1-\frac{1}{\cosh\sqrt{L_1^{(90)}}s}\right)}\ \frac{\overline{A}_{11}}{\overline{A}_{11}\overline{A}_{22}-\overline{A}_{12}^2} \tag{19}$$

From the energy perspective, formation of new cracks and increase of the crack density from D_i^{mc} to D_f^{mc} is possible if the following condition is fulfilled

$$-\Delta U = U_i - U_f \geq G_c \Delta A^{mc} \tag{20}$$

where U_i is the total strain energy stored in the laminate with the cracking density D_i^{mc}, U_f is the total strain energy stored in the laminate with the crack density D_f^{mc}, ΔA^{mc} is the increase in the total fracture area of multiple transverse cracks, and G_c (J/m^2) is the critical fracture toughness associated with matrix cracking, which could be taken as G_{Ic} if Mode I cracking is assumed.

The total strain energy stored in the laminate with the crack density D^{mc} can be calculated using the equivalent constraint laminate of the same length L and same width $2w$ as

$$U = \frac{1}{2} L(2w)\{\bar{\varepsilon}\}^T[\bar{A}]\{\bar{\varepsilon}\} \tag{21}$$

where the extension stiffness matrix of the equivalent constraint laminate $\bar{A}$ was defined in Eq. (15).

Given that D_i^{mc} and D_f^{mc} $(D_f^{mc} > D_i^{mc})$ are two discrete crack densities, the formulation given by Eq. (20) can be viewed as a *discrete formulation of the energy criterion*. In view of Eqs. (21) and (15), it can re-written as

$$\frac{1}{D_f^{mc} - D_i^{mc}} t_{90}\{\bar{\varepsilon}\}^T([R(D_f^{mc})] - [R(D_i^{mc})])\{\bar{\varepsilon}\} \geq G_c \tag{22}$$

If the area of a single crack is $a^{mc} = 4wt_{90}$, the total area covered by all cracks is equal to $A^{mc} = a^{mc}(2s)^{-1}L = 2wLD^{mc}$. Under the applied uniaxial strain $\bar{\varepsilon}_{22}$, Eqn. (22) simplifies to

$$\frac{1}{D_f^{mc} - D_i^{mc}} t_{90}\bar{\varepsilon}_{22}^2[b_0(D_f^{mc})\Lambda_{22}^{(90)}(D_f^{mc}) - b_0(D_i^{mc})\Lambda_{22}^{(90)}(D_i^{mc})] \geq G_c \tag{23}$$

where

$$b_0(D\ ) = \frac{\left(\hat{Q}_{22}^{(90)} - \frac{\overline{A}_{12}(D\ )}{\overline{A}_{11}(D\ )} \hat{Q}_{12}^{(90)} \right)^2}{\hat{Q}_{22}^{(90)}} \tag{24}$$

Since the coupled criterion requires the comparison of the stress and the energy criterion it is useful to express the condition in (23) in the same terms used for the stress criterion in Eq. (19). After some rearrangement the condition in (23) writes as,

$$\frac{\overline{\varepsilon}_{22}}{Y_{\varepsilon t}} \geq \gamma \sqrt{g_d(D_i^{mc}, D_f^{mc})} \tag{25}$$

where γ is a dimensionless brittleness number given by the following expression,

$$\gamma = \frac{1}{Y_t} \sqrt{\frac{G_c E_{22}}{t_{90}}} \tag{26}$$

and $g_d(D_i^{mc}, D_f^{mc})$ a dimensionless function which represents the ratio of dimensionless dissipated energy to dimensionless released energy,

$$g_d(D_i^{mc}, D_f^{mc}) = \frac{D_f^{mc} - D_i^{mc}}{[b_0(D_f^{mc})\Lambda_{22}^{(90)}(D_f^{mc}) - b_0(D_i^{mc})\Lambda_{22}^{(90)}(D_i^{mc})]/E_{22}} \tag{27}$$

For an increase in the number of cracks from N cracks to $N+1$ cracks, and the corresponding increase in crack density from D_N^{mc} and D_{N+1}^{mc}, the energy criterion can be formulated as

$$-\Delta U = U_N - U_{N+1} \geq G_c \Delta A^{mc} \tag{28}$$

Using Eqs. (21), (15), it can be re-written as

$$\frac{1}{D_{N+1}^{mc} - D_N^{mc}} t_{90} \{\overline{\varepsilon}\}^T ([R(D_{N+1}^{mc})] - [R(D_N^{mc})]) \{\overline{\varepsilon}\} \geq G_c \tag{29}$$

Under the applied uniaxial strain $\bar{\varepsilon}_{22}$, Eq. (29) simplifies to

$$\frac{1}{D_{N+1}^{mc}-D_N^{mc}} t_{90}\bar{\varepsilon}_{22}^2[b_0(D_{N+1}^{mc})\Lambda_{22}^{(90)}(D_{N+1}^{mc})-b_0(D_N^{mc})\Lambda_{22}^{(90)}(D_N^{mc})]\geq G_c \tag{30}$$

Replacing small increment with derivative yields *a continuum formulation of the energy criterion*

$$t_{90}\bar{\varepsilon}_{22}^2\frac{\partial\left(b_0\Lambda_{22}^{(90)}\right)}{\partial D^{mc}}\geq G_c, \tag{31}$$

which can be rewritten in the same terms as the discrete version,

$$\frac{\bar{\varepsilon}_{22}}{Y_{et}}\geq\gamma\sqrt{g_c(D^{mc})}, \tag{32}$$

with γ being given by Eq. (26) and the dimensionless function $g_c(D^{mc})$ as,

$$g_c(D^{mc})=\frac{E_{22}}{\frac{\partial\left(b_0\Lambda_{22}^{(90)}\right)}{\partial D^{mc}}}. \tag{33}$$

Lim and Li (2005) have shown, using the variation approach, that the difference between incremental and continuous expressions for the energy release rates associated with transverse cracking is negligible provided that the number of cracks N is large enough.

The present approach is in fact based on the assumption that the parameters used in the Coupled Criterion, as maximum stress value and released energy, are only weakly influenced by some irregularities in crack distribution. Actually, according to experimental observations at the beginning, for small crack densities, the crack distribution in real specimen may not be very regular, but for larger crack densities it becomes quite regular and the present approach could capture the real behavior accurately. Thus, we can expect that the predictions by the present approach will fit well the real growth of crack density variable for large values. However, for very

small crack densities values, some differences, associated to a random and irregular location of cracks and to other statistical effects like scattering in strength within the lamina, can appear.

5. Results and discussion

The stress criterion, expressed in condition (19), is represented in Figure 4 for carbon/epoxy. In the context of the discrete formulation, this figure shows the relation between the normalized applied strain and the initial and final crack densities, assuming the crack density is doubled when the conditions for the damage progress are fulfilled. The material is carbon/epoxy, with properties listed in Table 1, and $Y_{\varepsilon t}$ is the ultimate failure strain for transverse tension. For the continuous formulation the curve for the stress condition matches the curve for the discrete formulation which is function of the initial crack density. Observe that below a value of the applied strain no damage is expected because transverse stresses do not exceed the nominal unidirectional transverse strength of the lamina. Above a certain value the crack density grows with the applied strain.

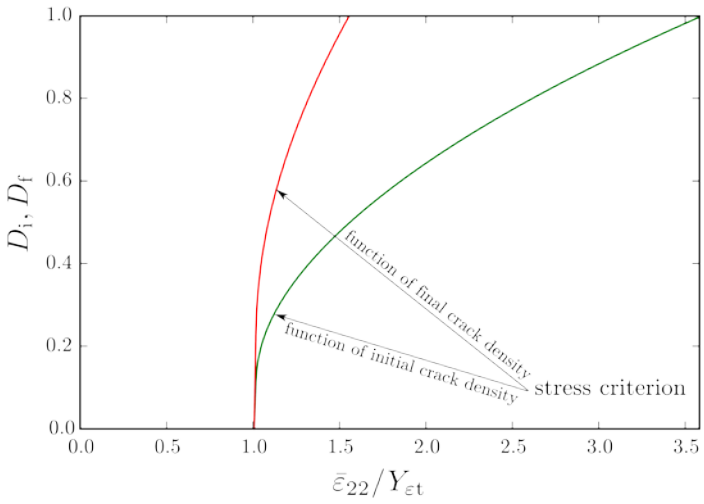

Figure 4. Stress criterion: Relative crack density $D^{mc} = t_{90}/s$ as a function of the applied strain $\bar{\varepsilon}_{22}/Y_{\varepsilon t}$ for carbon/epoxy and $t_0/t_{90} = 1$.

The energy criterion, expressed in Eqns. (25) and (32), is represented in Figure 5. The two formulations of the energy criterion are examined. Figure 5a-f shows the normalized crack density $D^{mc} = t_{90}/s$ versus the normalized applied strain $\bar{\varepsilon}_{22}/Y_{\varepsilon t}$ as predicted by the discrete and continuous energy criteria, for a range of brittleness numbers $\gamma = \sqrt{E_T G_c / t_{90}}\,/Y_t$ and carbon/epoxy.

Brittleness number γ, introduced by Mantič (2009) into the framework of FFM and specified for this problem by Garcia et al (2014), is a structural parameter that characterizes the transition from brittle to tough configurations by a suitable combination of stiffness, strength, fracture toughness and transverse layer thickness in a laminate. It can be viewed as a generalization to orthotropic materials of Carpinteri's brittleness number introduced initially for isotropic materials (Carpinteri, 1982). It can be observed from Fig 4 that the energy criterion curves shift upward with increasing γ. This is due to the fact that the values of the critical strain predicted by the energy criterion are actually directly proportional to γ (cf. Garcia et al, 2014). This can be viewed as a size effect where the predicted critical strain is inversely proportional to the square root of the transverse layer thickness t_{90}.

Table 1. Elastic properties and thickness of composite laminates.

Material	E_L (GPa)	E_T (GPa)	ν_{LT}	G_{LT}(GPa)	t (mm)
Carbon/epoxy (Zhang, Fan and Soutis, 1992a)	144.8	11.38	0.3	6.48	0.150
Glass/epoxy (Parvizi et al, 1978)	42	14	0.278	5.83	0.150
SiC/CAS (Soutis and Kashtalyan, 2011)	121	112	0.2	44	0.150

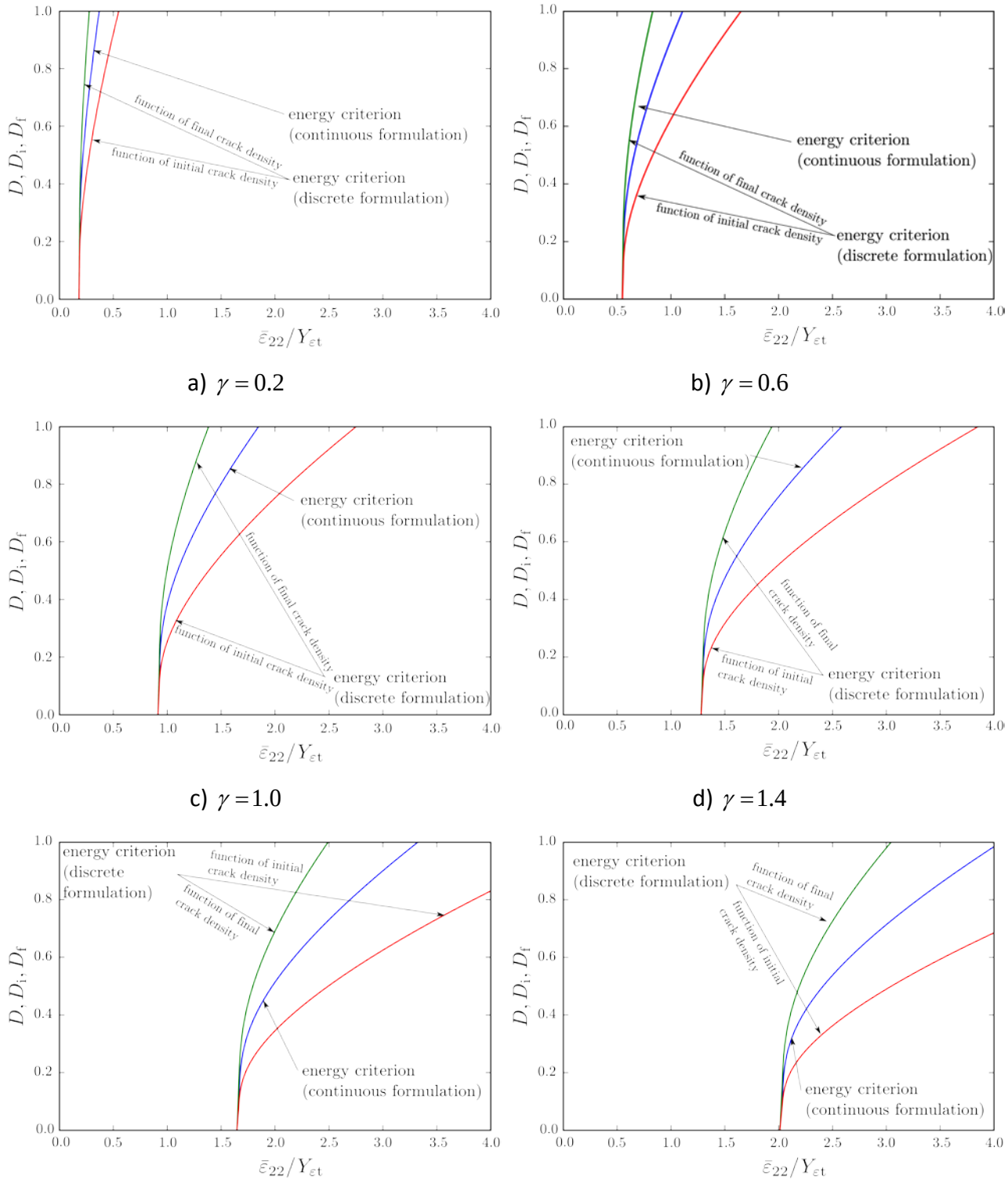

Figure 5. Energy criterion: Relative crack density $D^{mc} = t_{90}/s$ as a function of the normalised applied strain $\bar{\varepsilon}_{22}/Y_{\varepsilon t}$ for carbon/epoxy and $t_0/t_{90} = 1$.

In the discrete formulation, doubling of the relative crack density is assumed, i.e. $D_f^{mc} = 2D_i^{mc}$. The assumption of doubling the number of cracks is also used in Garrett and Bailey (1977), Nairn (2000) and Leguillon et al (2017). Thus, for any given crack density $D^{mc} \equiv D_i^{mc}$, the discrete energy criterion estimates conditions for doubling that crack density. In contrast, the continuous energy criterion estimates conditions, under which, for any given D^{mc}, just one new crack would appear. Both criteria predict an increase in the transverse crack density with the applied strain as expected, with the curve for the continuous formulation of the energy criterion lying between the curves for the discrete formulation (expressed as a function of the initial and final crack density). This has been proved in Appendix A and is a very relevant result because it explains why the continuous formulation of related approaches, widely used in the literature, see e.g. Hashin (1996), obtains a good agreement with experiments despite the inherent discrete nature of the process. In addition, as has been also proved in Appendix A, for small values of the relative crack density the two energy criteria are very close in their predictions, however as the crack density becomes larger they diverge from one another.

To clarify the relationship between the discrete and continuous formulation, some possible crack density evolution according to the discrete formulation for different initial values of the crack density are plotted in Figure 6. As can be noticed the two curves corresponding to the discrete formulation represents the boundary of a region which encloses the possible paths for crack density progression. As can be observed these possible paths depend strongly on the initial crack density. Thus, the entire region between the two curves should be taken for prediction purposes. In this context, the continuous formulation, used in other works applying only the energy criterion, lies here in the middle of the region of possible states.

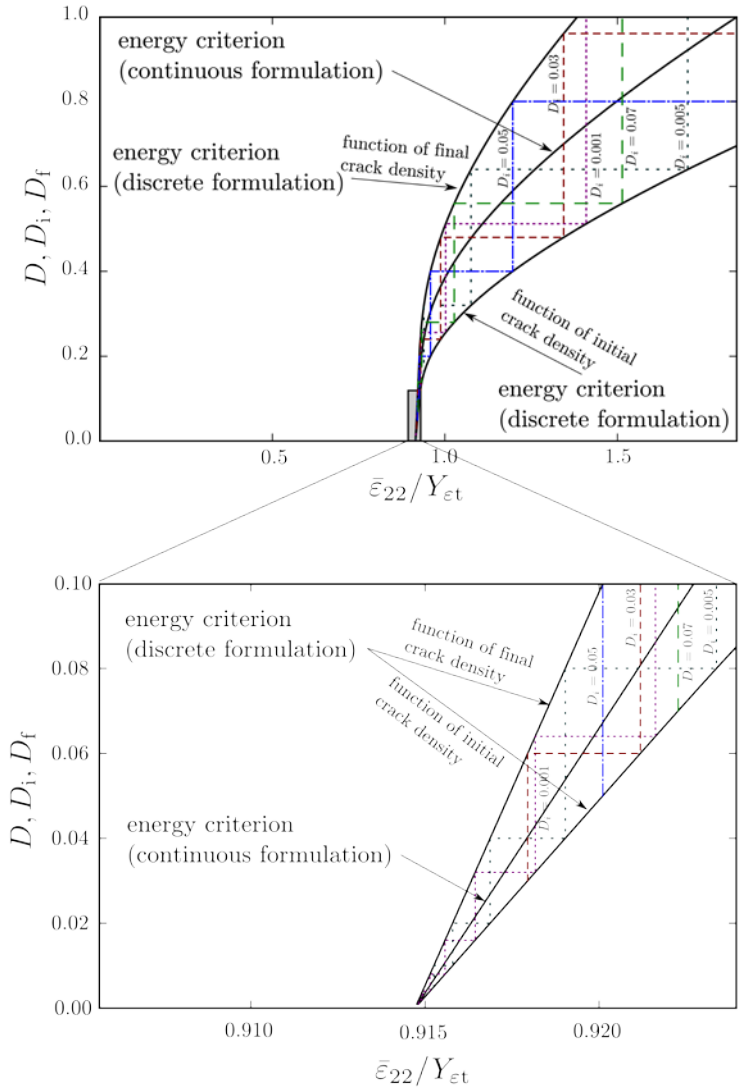

Figure 6. Energy criterion: Crack density evolution predicted by the discrete formulation for different values of the initial crack density and carbon/epoxy and $t_0 / t_{90} = 1$.

When applying the Coupled Criterion of FFM, the energy criterion is combined with the stress criterion. According to Leguillon's hypothesis (Leguillon, 2002), the fracture event (in this case, the evolution of crack density) is governed by the more restrictive of the stress and energy criteria in each situation (in this case, for each value of the damage parameter D_i^{mc} or D^{mc}).

Figure 7a-f shows the relative crack density $D^{mc} = t_{90} / s$ versus the normalized applied strain $\bar{\varepsilon}_{22} / Y_{\varepsilon t}$ as predicted by the coupled criterion comprising the stress criterion (SC) and the continuous energy criterion (EC), for a range of brittleness number γ values and for three composites whose properties are listed in Table 1. We observe that for brittleness numbers $\gamma = 0.2$ (Fig. 7a), $\gamma = 0.6$

(Fig. 7b), and $\gamma = 1.0$ (Fig. 7c), the coupled criterion is dominated by the stress criterion, which appears to be more restrictive for the three material systems. However, for example, when $\gamma = 1.4$ (Fig. 7d), the dominance switches from the stress criterion to the energy criterion for carbon/epoxy and glass/epoxy for certain values of crack densities. This transition happens at approximately $D^{mc} \approx 0.45$. For the brittleness number $\gamma = 1.8$ (Fig. 5e), the transition point is at $D^{mc} \approx 0.8$ for carbon/epoxy laminate and at $D^{mc} \approx 0.9$ for glass/epoxy system. For higher values of brittleness number $\gamma = 2.2$ (Fig. 7f), the coupled criterion is dominated by the energy criterion for the three material systems.

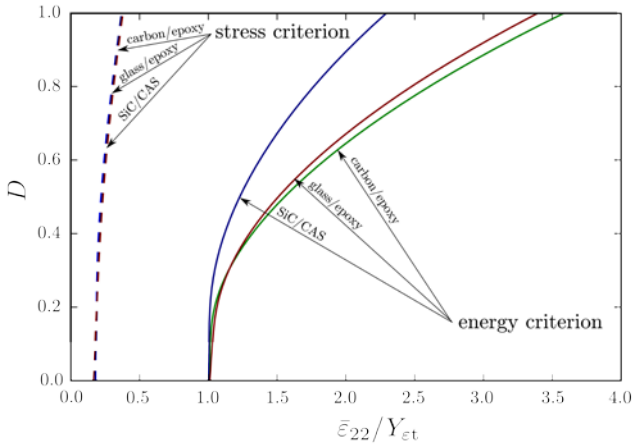

a) $\gamma = 0.2$

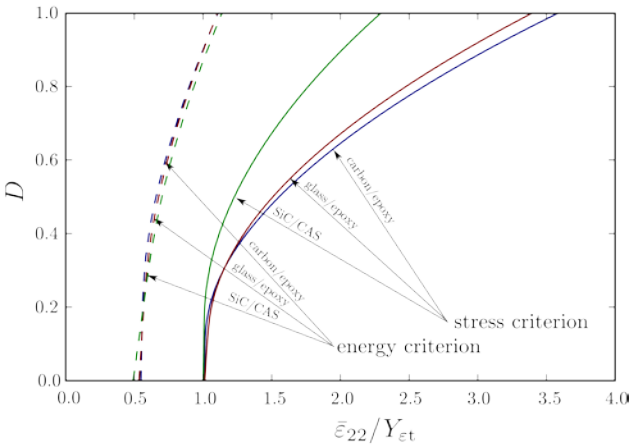

b) $\gamma = 0.6$

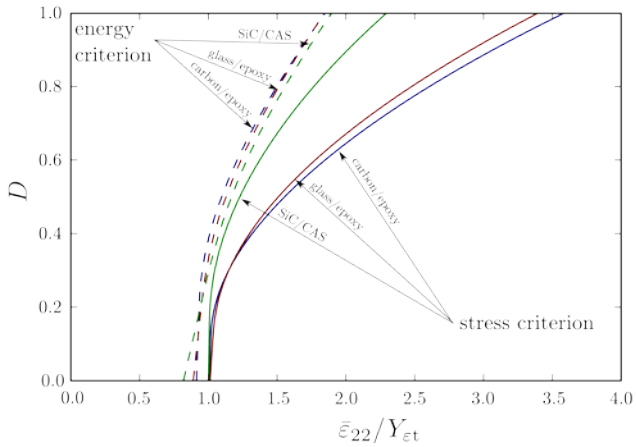

c) $\gamma = 1.0$

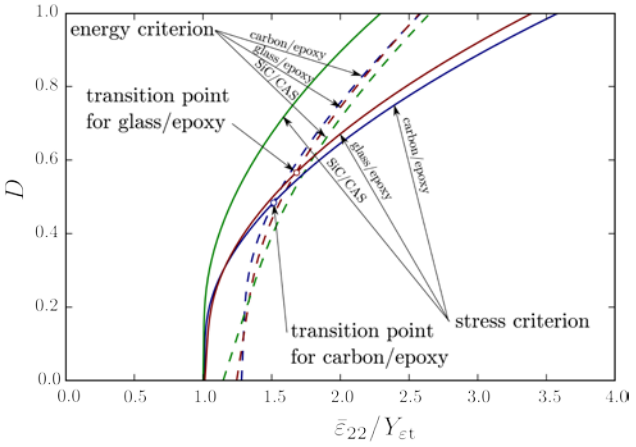

d) $\gamma = 1.4$

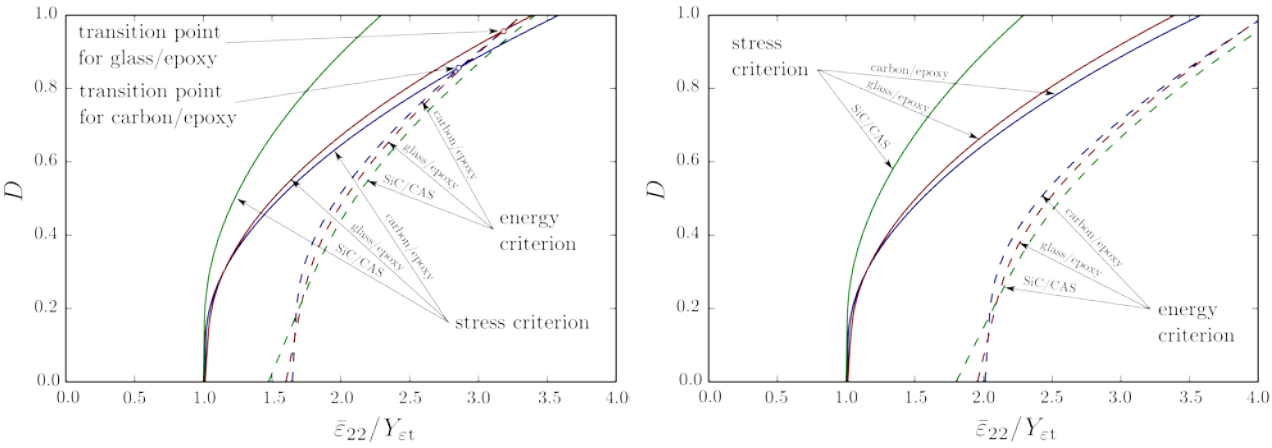

e) $\gamma = 1.8$ f) $\gamma = 2.2$

Figure 7. Relative crack density as a function of the normalized applied strain, as predicted by the stress criterion (SC) and the continuous formulation of the energy criterion (EC) for $t_0 / t_{90} = 1$ and three composites whose properties are listed in Table 1.

Figure 8a-d shows dependence of the relative crack density $D^{mc} = t_{90} / s$ on the normalized applied strain $\bar{\varepsilon}_{22} / Y_{\varepsilon t}$, as predicted by the Coupled Criterion, using the continuous formulation, for a range of layer thickness ratios t_0 / t_{90}. The material system is carbon/epoxy. As can be seen from Fig. 8a-d, the Coupled Criterion predictions match for $\gamma = 0.2; 0.6; 1.0$ for all considered layer thickness ratios. The reason for this is that in this situation the failure is governed by the stress criterion. For $\gamma = 1.4$, a clear transition from the energy criterion to the stress criterion within the coupled criterion is observed, while for $\gamma = 1.8; 2.2$, the coupled criterion is dominated by the energy criterion. As can be observed the curves are very similar when varying the layer thickness ratio t_0 / t_{90}, showing a weak influence of this parameter.

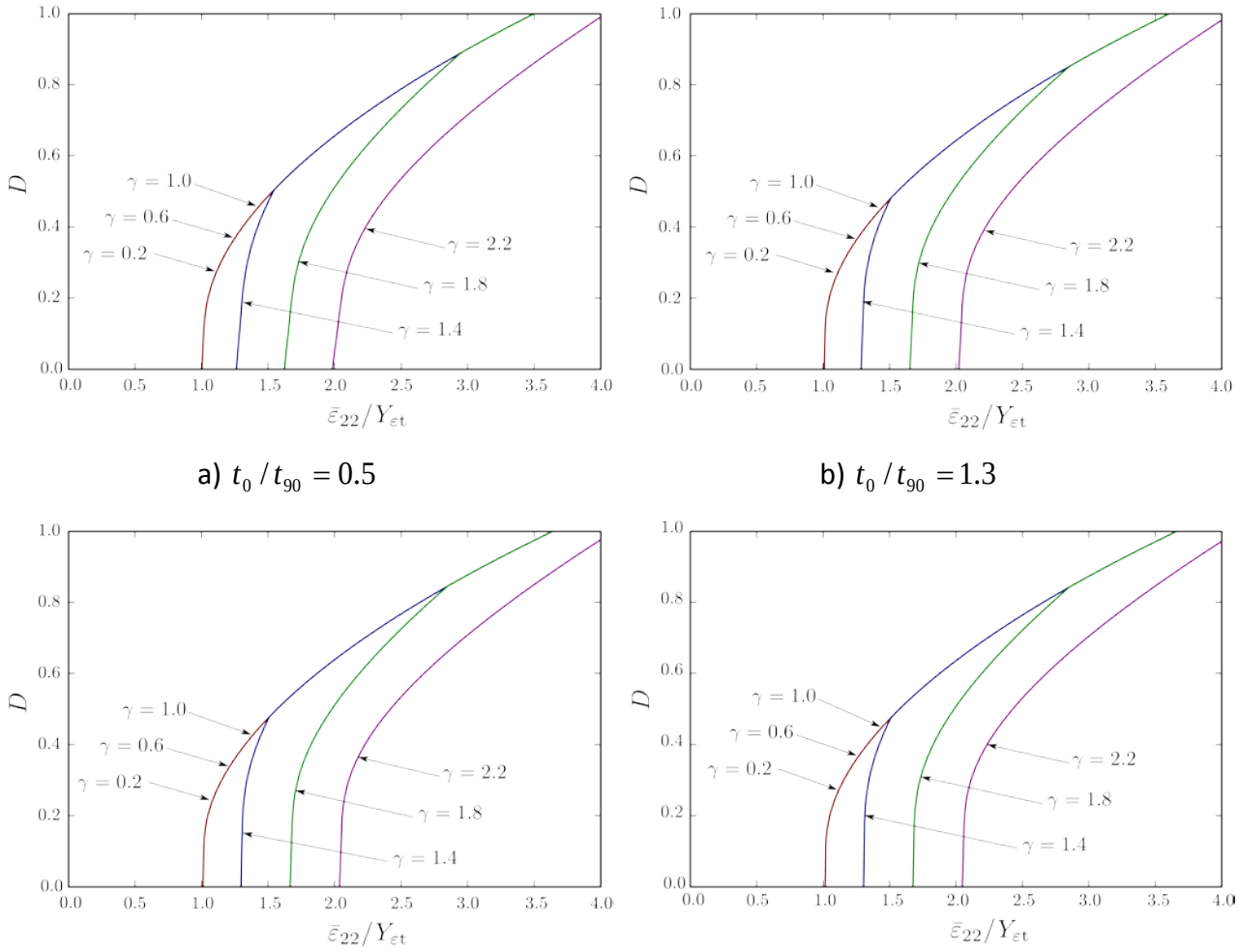

a) $t_0/t_{90} = 0.5$ b) $t_0/t_{90} = 1.3$

c) $t_0/t_{90} = 2.1$ d) $t_0/t_{90} = 2.9$

Figure 8. Relative crack density as a function of the normalized strain as predicted by the coupled criterion, for a range of layer thickness ratios and carbon/epoxy.

Comparison with experimental data of Nairn (2000)

Nairn (2000) plots crack density (in 1/mm) as a function of stress. To enable a preliminary comparison with our predictions, which show relative crack density as a function of normalized applied strain, we assume that stresses in Nairn's (2000) curves correspond to the applied stress (i.e. applied force divided by the total cross-sectional area of the specimen). The change is carried out using Eqn. (16). The strength data for AS4/3506-1 are from Soden et al. (1998).

Figure 9 presents the comparison between Nairn´s experiments and the model presented here. The comparison shows a good agreement for moderate and high values of the crack density in all laminates. Below a certain damage level $D \approx 0.25$ the model overestimates the strain level necessary for the progress of the crack density. This disagreement is likely due to the presence of

defects which generate premature transverse cracks. This idea suggests the need of including the randomness of the strength and fracture properties in the model. Although the damage level below which the prediction fails it is independent of the laminate thickness, in terms of the final damage level the damage interval for which the model fails is more relevant for the thinnest laminates.

The three laminates studied by Nairn correspond to a) $\gamma = 4.38$, b) $\gamma = 3.09$ and c) $\gamma = 2.19$, all being governed by the energy criterion. It would be interesting to compare with experiments of thicker laminates which corresponds to low values of gamma governed by the stress criterion. The stress criterion has been shown to be essential to explain transverse crack initiation, so it is foreseeable to be relevant for the whole transverse cracking process.

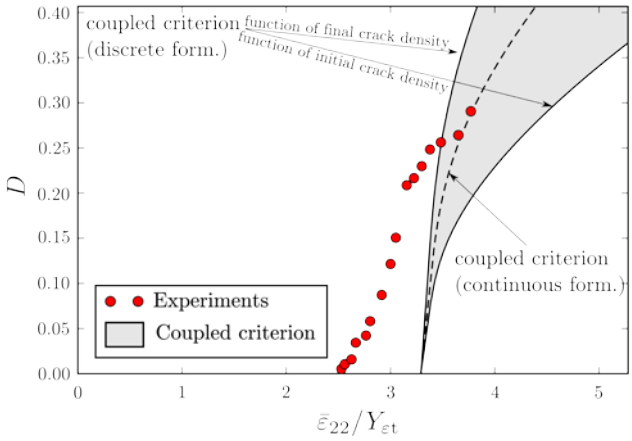

a) $[0/90]_s$

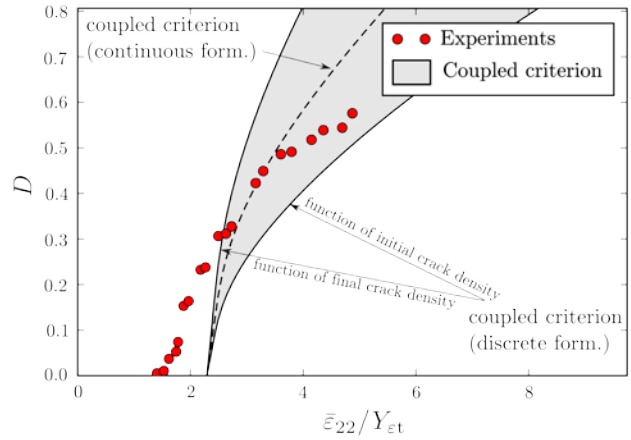

b) $[0/90_2]_s$

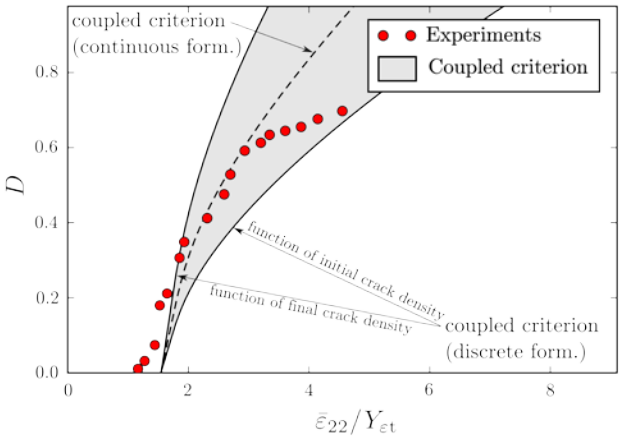

c) $[0/90_4]_s$

Figure 9. Comparison of predictions by the model generated here with the experiments by Nairn (2000).

Concluding remarks

A new model to predict crack density evolution in cross-ply laminates subjected to tension is presented. Closed-form expressions for the evaluation of the criteria involved are provided thanks to the combination of the Equivalent Constraint Model and the Coupled Criterion of the Finite Fracture Mechanics. In addition this model can be evaluated using only some material properties which can be easily measured using well established standards as the typical elastic properties, transverse strength and transverse fracture toughness.

It should be mentioned that for analysis of multiple matrix cracking in cross-ply laminate, the Coupled Criterion of FFM, combined here with the ECM, can be also used with any other method for stress analysis and released energy evaluation, for example, with variational approaches such as Nairn's (2000) or finite element modelling such as in Leguillon et al. (2017), Li and Leguillon (2017).

The discrete formulation of the energy criterion, with the assumption of doubling crack density lead to similar step-wise predictions of crack density evolution with the applied strain as presented by Leguillon et al. (2017). All possible paths for crack density progression have been demonstrated to be enclosed by the two curves of the discrete energy which are referred to the initial and the final crack density. Thus, the region of possible states between the two curves should be a good prediction.

The first comparison with experiments shows a good agreement except for low values of the crack density, likely due to the presence of defects generating premature transverse cracking leading to

initially somewhat irregular crack distribution. This could be solved by including the effect of randomness in strength and fracture properties. In addition, in this paper, we assumed that matrix cracks are spaced uniformly, however, in reality this is not always the case. Small variations in the uniformity of crack distribution should not affect the predictions, but in general the effect of randomness needs to be taken into account when predicting initiation of matrix, see Li and Wisnom (1997), Wisnom (2000). However a new model including the randomness effect would require additional material properties which need extensive test campaigns. This fact would reduce the usability of the model proposed.

Acknowledgements

The authors are indebted to Professors Federico París and Antonio Blázquez (University of Seville) for inspiring discussions. The authors wish to thank the Royal Society (UK) International Exchanges Scheme (award # IE141234), the Spanish Ministry of Economy and Competitiveness and European Regional Development Fund (Projects MAT2012-37387 and MAT2015-71036-P) for supporting this research.

Appendix A. Proof of the relation between the different energy criteria

The objective of this appendix is to show the relationship between the different curves representing the energy criteria in Figure 5. The curve corresponding to the energy criterion in the continuous formulation, Eqn. (31), is given by the derivative of the dimensionless strain energy (1-$b_0\Lambda_{22}^{(90)}$) with respect to the crack density. Figure A.1 shows the dimensionless strain energy as a function of the crack density for carbon/epoxy, which is a convex curve, as expected. Thus, the derivative implicated in the continuous formulation corresponds to the slope of the tangent to this curve. For comparison with the discrete formulation, we focus on a certain value $D = D_0$. The discrete formulation is based on the difference between two energetic states divided over the jump of crack density, see Eq. (23). In Figure A.1 this value corresponds to the slope of the secant between $D = D_0$ and $D = 2D_0$ if the energy criterion is expressed as a function of the initial crack density or between $D = D_0 / 2$ and $D = D_0$ if the criterion is expressed as a function of the final crack density. As can be observed in Figure A1 the slope of the tangent (giving the continuous formulation of the energy criterion) lies between the slopes of the two secants (giving the two curves for the discrete formulation) due to the convexity of the curve. As a consequence the curve corresponding to the continuous formulation of the energy criterion lies between the two curves

of the discrete formulation as can be observed in Figure 5. In addition, for lower values of the crack density the difference between the slopes will be lower because the jumps and the curvature will be smaller. Thus, the three curves tend to the same point for vanishing crack density as can be observed in Figure 5.

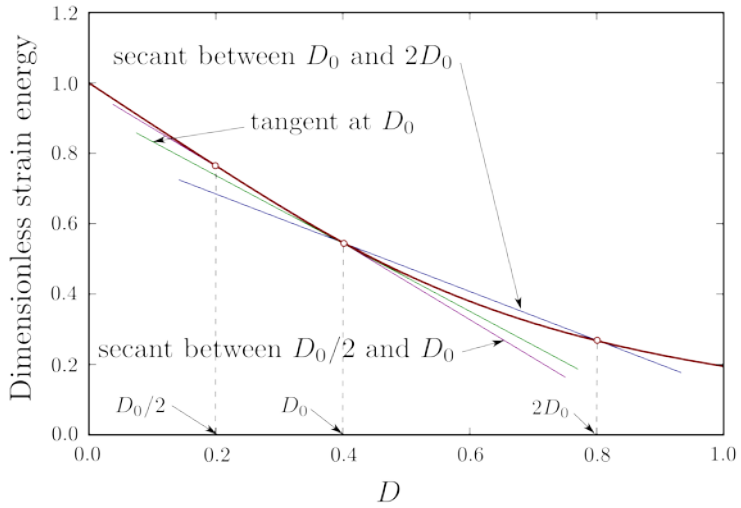

Figure A1. Dimensionless strain energy as a function of the normalized crack density.

References

Arteiro, A., Catalanotti, G., Melro, A.R., Linde, P., Camanho, P.P. (2014) Micro-mechanical analysis of the effect in polymer composite laminates, Composite Structures 116, , 827-840.

Berthelot, J. (2003) Transverse cracking and delamination in cross-ply glass-fiber and carbon–fiber reinforced plastic laminates: static and fatigue loading. Appl. Mech. Rev. 56 (1), 111–147

Carpinteri, A., (1982) Notch sensitivity in fracture testing of aggregative materials.Engineering Fracture Mechanics 16, 467–481.

Caslini, M., Zanotti, C., and O'Brien, T. (1987) Study of Matrix Cracking and Delamination in Glass/Epoxy Laminates, Journal of Composites, Technology and Research 9, 121-130.

García, I.G., Mantič, V., Blázques, A., Paris, F. (2014) Transverse crack onset and growth in cross-ply $[0/90]_s$ laminates under tension. Application of a coupled stress and energy criterion. International Journal of Solids and Structures 51: 3844–3856.

Garrett, K.W., Bailey, J.E (1977) Multiple transverse fracture in 90º cross-ply laminates of a glass fibre-reinforced polyester. Journal of Materials Science 12: 157-168.

Hashin, Z. (1996) Finite thermoelastic fracture criterion with application to laminate cracking analysis. Journal of the Mechanics and Physics of Solids 44: 1129-1145.

Herráez, M., Mora, D., Naya, F., Lopes, C.S., González, C., LLorca, J. (2015) Transverse cracking of cross-ply laminates: A computational micromechanics perspective, Composites Science and Technology,110, 196-204.

Kashtalyan, M., Soutis, C (2000) Stiffness degradation in cross-ply laminates damaged by transverse cracking and splitting. Composites Part A: Applied Science and Manufacturing 31: 335-351.

Kashtalyan, M., Soutis, C. (2005) Analysis of composite laminates with intra- and interlaminar damage. Progress in Aerospace Sciences 41: 152-173.

Kashtalyan, M., Soutis, C. (2006) Modelling off-axis ply matrix cracking in continuous fibre-reinforced polymer matrix composite laminates. Journal of Materials Science 41: 6789-6799.

Kashtalyan, M., Soutis, C. (2013) Predicting residual stiffness of cracked composite laminates subjected to multi-axial in-plane loading. Journal of Composite Materials 47: 2513-2524.

Laws, N., Dvorak, G. (1988) Progressive transverse cracking in composite laminates. Journal of Composite Materials 22: 900-916.

Leguillon, D. (2002) Strength of toughness? A criterion for crack onset at a notch. European Journal of Mechanics A/ Solids 21:61–72.

Leguillon, D., Li, J., Martin, E. (2017) Multi-cracking in brittle thin layers and coatings using a FFM model. European Journal of Mechanics A/ Solids 63: 14-21.

Li, J., Leguillon, D. (2017) Finite element implementation of the coupled criterion for numerical simulations of crack initiation and propagation in brittle materials, Theoretical and Applied Fracture Mechanics (In press) DOI: http://dx.doi.org/10.1016/j.tafmec.2017.07.010.

Li, D.S., Wisnom, M.R. (1997) Evaluating Weibull parameters for transverse cracking in cross-ply laminates. Journal of Composite Materials 31: 935-951.

Lim, S.H., Li, S. (2005) Energy release rates for transverse cracking and delaminations induced by transverse cracks in laminated composites. Composites Part A: Applied Science and Manufacturing 36: 1467-1476.

Mantič, V. (2009) Interface crack onset at a circular cylindrical inclusion under transverse tension. Application of a coupled stress and energy criterion. International Journal of Solids and Structures 46: 1287-1304.

Mantič, V., García, I.G. (2012) Crack onset and growth at the fibre-matrix interface under a remote biaxial transverse load. Application of a coupled stress and energy criterion. International Journal of Solids and Structures 40: 2273-2290.

Nairn, J.A. (1989) The strain energy release rate for composite microcracking: A variational approach. Journal of Composite Materials 23: 1106-

Nairn, J.A. (2000) Matrix cracking in composites. In A. Kelly, C. Zweben (Eds.) Comprehensive Composite Materials, Volume 2, pp. 403-432. Oxford: Pergamon.

Parvizi, A., Garrett, K., Bailey, J. (1978) Constrained cracking in glass fibre-reinforced epoxy cross-ply laminates. J. Mater. Sci. 13, 195-201.

Saito, H., Takeuchi, H., Kimpara, I. (2014) A study of crack suppression mechanism ofthin-ply carbon-fiber-reinforced polymer laminate with mesoscopicnumerical simulation, Journal of Composite Materials 48 (17), 2085–2096.

Silberschmidt, V.V. (2005). Matrix cracking in cross-ply laminates: effect of randomness. Composites Part A 36: 129-135.

Singh, C.V. (2016) Evolution of multiple matrix cracking. In: Modeling Damage, Fatigue and Failure of Composite Materials (eds R Talreja and J Varna). Cambridge: Woodhead Publishing.

Soden, P.D., Hinton, M.J., Kaddour,A.S. (1998) Lamina properties, lay-up configurations and loading conditionsfor a range of fibre-reinforced composites laminates. Composite Science and Technology 58: 1011-1022.

Soutis, C., Kashtalyan, M. (2011) Residual stiffness of cracked cross-ply laminates under multiaxial in-plane loading. Applied Composite Materials 18: 31-43.

Távara, L., Reinoso, J., Castillo, D., Mantič, V., Mixed-mode failure of interfaces studied by the 2D Linear Elastic-Brittle Interface Model: macro- and micro-mechanical finite element applications in composites. The Journal of Adhesion. DOI: http://dx.doi.org/10.1080/00218464.2017.1320988

Weiβgraeber, P., Leguillon, D., Becker, W. (2016) A review of Finite Fracture Mechanics: crack initiation at singular and non-singular stress raisers. Archive of Applied Mechanics 86: 375-401.

Wisnom, M.R. (2000) Size effects in composites. In Kelly, A., Zweben, C. (Eds), Comprehensive Composite Materials, vol. 2. Pergamon, Oxford, pp. 23-47.

Zhang, J., Fan, J., Soutis, C. (1992a) Analysis of multiple transverse cracking in $[\pm\theta_m/90_n]_s$ composite laminates Part 1: In-plane stiffness properties. Composites 23: 291-298.

Zhang, J., Fan, J., Soutis, C. (1992b) Analysis of multiple transverse cracking in $[\pm\theta_m/90_n]_s$ composite laminates Part 2: Development of transverse cracks. Composites 23: 299-311.